Journal of Insect Physiology 55 (2009) 599–607

Contents lists available at ScienceDirect

Journal of Insect Physiology

journal homepage: www.elsevier.com/locate/jinsphys

K^+ homeostasis and central pattern generation in the metathoracic ganglion of the locust

Corinne I. Rodgers *, John D. LaBrie, R. Meldrum Robertson

Department of Biology, Queen's University, Biosciences Complex, Kingston, Ontario, Canada K7L 3N6

ARTICLE INFO

Article history:
Received 16 December 2008
Received in revised form 27 February 2009
Accepted 9 March 2009

Keywords:
Central pattern generator
Locust
Na^+/K^+-ATPase
Potassium
Spreading depression

ABSTRACT

Stress-induced arrest of ventilatory motor pattern generation is tightly correlated with an abrupt increase in extracellular potassium concentration ($[K^+]_o$) within the metathoracic neuropil of the locust, *Locusta migratoria*. Na^+/K^+-ATPase inhibition with ouabain elicits repetitive surges of $[K^+]_o$ that coincide with arrest and recovery of motor activity. Here we show that ouabain induces repetitive $[K^+]_o$ events in a concentration-dependent manner. 10^{-5} M, 10^{-4} M, and 10^{-3} M ouabain was bath-applied in semi-intact locust preparations. 10^{-4} M and 10^{-3} M ouabain reliably induced repetitive $[K^+]_o$ events whereas 10^{-5} M ouabain had no significant effect. In comparison to 10^{-4} M ouabain, 10^{-3} M ouabain increased the number and hastened the time to onset of repetitive $[K^+]_o$ waves, prolonged $[K^+]_o$ event duration, increased resting $[K^+]_o$, and diminished the absolute value of $[K^+]_o$ waves. Recovery of motor patterning following $[K^+]_o$ events was less likely in 10^{-3} M ouabain. In addition, we show that K^+ channel inhibition using TEA suppressed the onset and decreased the amplitude of ouabain-induced repetitive $[K^+]_o$ waves. Our results demonstrate that ventilatory circuit function in the locust CNS is dependent on the balance between mechanisms of $[K^+]$ accumulation and $[K^+]$ clearance. We suggest that with an imbalance in favour of accumulation the system tends towards a bistable state with transitions mediated by positive feedback involving voltage-dependent K^+ channels.

1. Introduction

Potassium (K^+) plays an important role in the nervous system and therefore disruption of K^+ homeostasis can have important consequences for neuronal function. Prior research using both invertebrate and vertebrate models has demonstrated that stress-induced failure of neural function coincides with a loss in K^+ homeostasis (Rounds, 1967; Erulkar and Weight, 1977; Balestrino et al., 1999; Wu and Fisher, 2000; Xiong and Stringer, 2000; Rodgers et al., 2007). In the locust (*Locusta migratoria*) stress-induced arrest of ventilation is tightly correlated with an abrupt increase in extracellular potassium concentration ($[K^+]_o$) within the ventilatory neuropil (Rodgers et al., 2007), however the cellular mechanisms involved in the initiation of and recovery from stress-induced ventilatory arrest and the associated increases in $[K^+]_o$ in the locust are not known. We investigated the role of the Na^+/K^+ pump and K^+ channel conductances in ventilatory arrest and recovery.

The migratory locust provides an exceptional model system for characterizing the relationship between neural circuit function and K^+ ion homeostasis. This invertebrate provides a rare opportunity as its vital neural circuitry is experimentally accessible for simultaneous, comprehensive studies at both cellular and systemic levels (Robertson, 2004). We are able to monitor potassium ion disturbances within the neuropil while simultaneously monitoring failure and recovery of an intact neural circuit. Ventilation is a key motor behaviour necessary for the circulation, supply, and removal of respiratory gases. Due to its important nature it is imperative that functioning remains intact, as prolonged loss of function could lead to oxygen starvation and ultimately death. Ventilation, defined as the contraction and expansion of the thoracic and abdominal cavities, is represented by two different forms in the locust: discontinuous and continuous (Harrison, 1997; Bustami and Hustert, 2000). Whereas discontinuous ventilation commonly occurs during undisturbed states or rest (Harrison, 1997), stress causes the ventilatory pattern to become continuous, making ventilatory muscles contract in a more constant and predictable fashion (Bustami and Hustert, 2000). Control of ventilatory motor activity in locusts is accomplished by a central pattern generator (CPG) situated in the metathoracic ganglion (MTG) (Ramirez and Pearson, 1989; Bustami and Hustert, 2000). Although incomplete, current knowledge indicates that the

* Corresponding author.
E-mail address: corinne.rodgers@queensu.ca (C.I. Rodgers).

Abbreviations: CPG, central pattern generator; $[K^+]_o$, extracellular potassium concentration; $[Na^+]_i$, intracellular sodium concentration; MTG, metathoracic ganglion; SD, spreading depression; vCPG, ventilatory central pattern generator.

0022-1910/$ – see front matter © 2009 Elsevier Ltd. All rights reserved.
doi:10.1016/j.jinsphys.2009.03.004

ventilatory CPG (''vCPG'') is composed primarily of a network of interneurons (Ramirez and Pearson, 1989), which are connected to the motor neurons relaying neuronal signals to the thoracic and abdominal muscles responsible for ventilation (Bustami and Hustert, 2000).

Neuronal membranes become depolarized when $[K^+]_o$ increases (Huxley and Stämpfli, 1951; Somjen, 2002). Initially, a neuron can become hyperexcitable as its firing threshold is approached during minor depolarization (Balestrino et al., 1999; Somjen, 2002). Further depolarization however can depress excitability as some voltage-gated Na^+ and Ca^{2+} channels inactivate, which increases firing threshold, decreases action potential amplitude, and can also limit neurotransmitter release (Erulkar and Weight, 1977; Somjen, 2002). $[K^+]_o$ levels are largely regulated by glial cells which form the superficial layer of the insect CNS, also referred to as the sheath of the ganglion (Kretzschmar and Pflugfelder, 2002). Glial cells utilize multiple different ion channels that are capable of K^+ uptake from the interstitial space. The $Na^+/K^+/2Cl^-$ co-transporter, for instance, picks up a K^+ ion from the extracellular space in exchange for a Na^+ ion and two Cl^- ions (Walz, 1987), while inwardly rectifying potassium channels have been shown to display an increase in conduction during rises in $[K^+]_o$ (Newman, 1993; Leis et al., 2005). In addition, gap junctions between glial cells provide a network that acts as a ''spatial buffer'' for K^+ (Orkand et al., 1966; Leis et al., 2005). The Na^+/K^+-ATPase is essential for cellular function due to its role in maintenance of ionic concentration gradients across the membrane. The Na^+/K^+-ATPase has a hyperpolarizing effect in cells by pumping three Na^+ ions out of the cell for every two K^+ ions into the cell and this requires the expenditure of energy (ATP hydrolysis). 50–60% of neuronal ATP levels are devoted to driving the Na^+/K^+ pump (Erecinska and Silver, 1994) indicating its important role in the maintenance of ion homeostasis.

Previously we have shown that in the locust abrupt increases in $[K^+]_o$ are reliably triggered in response to multiple cellular stressors, namely hyperthermia, anoxia (N_2), ATP depletion (NaN_3), and Na^+/K^+-ATPase impairment (ouabain) (Rodgers et al., 2007). The increase in $[K^+]_o$ associated with arrest of the ventilatory motor pattern occurs within the locust MTG surrounding the vCPG and is not modest, increasing by approximately 40–60 mM at arrest induced by anoxia, ATP depletion, and Na^+/K^+-ATPase inhibition (Rodgers et al., 2007). $[K^+]_o$ gradually decreases when the stress is removed and this coincides with recovery of ventilatory motor pattern generation (Rodgers et al., 2007). Interestingly, inhibition of the Na^+/K^+ pump induces repetitive arrest of the vCPG (Rodgers et al., 2007). Continuous bath application of 10^{-4} M ouabain elicits multiple surges in $[K^+]_o$ where the rise and fall of $[K^+]_o$ are associated with arrest and recovery of the ventilatory motor pattern, respectively (Rodgers et al., 2007). One explanation for the repetitive nature of the arrest induced by 10^{-4} M ouabain is that it critically depends on the balance between the processes of $[K^+]_o$ accumulation and clearance. If this hypothesis is true then manipulation of these processes should affect the occurrence and characteristics of repetitive ventilatory arrest.

In this paper we characterize ouabain-induced repetitive $[K^+]_o$ events in the locust ventilatory neuropil and the associated vCPG arrest in detail. We show that the time to initiation as well as the severity of this phenomenon, i.e. number of $[K^+]_o$ events, $[K^+]_o$ event duration, pre- and post-surge resting $[K^+]_o$ levels, slope of $[K^+]_o$ increase, and likelihood of vCPG recovery following $[K^+]_o$ surges, is dependent on the magnitude of ouabain-induced inhibition of $[K^+]_o$ clearance (varying ouabain concentration). We also show that the onset and severity of repetitive $[K^+]_o$ events induced by ouabain is dependent on the level of $[K^+]_o$ accumulation through K^+ channels (inhibition of voltage-dependent K^+ channels with tetraethylammonium chloride (TEA)).

2. Materials and methods

2.1. Animals

Adult male locusts, *L. migratoria migratorioides* (R. and F.), aged approximately 3–5 weeks past imaginal ecdysis, were randomly selected from a crowded colony located in the Animal Care Facility of the Biosciences Complex at Queen's University. The colony was reared under a 12 h:12 h light:dark photoperiod at a room temperature of 30 ± 1 °C during light hours and 26 ± 1 °C during dark hours. Humidity was maintained at 23 ± 1%. Animals were provided with carrots, wheat seedlings and an ad libitum mixture of 1 part skim milk powder, 1 part torula yeast, and 13 parts bran, by volume.

2.2. Preparation of potassium-sensitive microelectrodes

K^+-sensitive microelectrodes were made from 1 mm diameter unfilamented capillary tubes (World Precision Instruments Inc., Sarasota, FL, USA) that were cleaned with methanol (99.9%) and dried on a hot plate before being pulled to form a low resistance (5–7 MΩ) tip. The inner glass surface of the microelectrodes was made hydrophobic by exposure to dichlorodimethylsilane (99%) (Sigma–Aldrich) vapor while baking on a hot plate (100 °C) for 1 h. The microelectrodes were allowed to cool, then filled at the tip with Potassium Ionophore I-Cocktail B (5% valinomycin; Sigma–Aldrich) and back-filled with 500 mM KCl. Reference microelectrodes were made from 1 mm diameter filamented capillary tubes (World Precision Instruments Inc., Sarasota, FL, USA) that were pulled to form a low resistance (5–7 MΩ) tip, then filled with 3 M KCl. Microelectrode tips were suspended in distilled water until experimentation.

2.3. Semi-intact preparation

Appendages and pronotum were removed and a dorsal midline incision was made. A corkboard was used to pin open the locust dorsal side up, allowing the gut, fatty tissue and air sacs to be removed, exposing the metathoracic ganglion (MTG) and ventilatory muscle 161 (M161) found in the second abdominal segment (A2). This provided a semi-intact preparation as utilized by Newman et al. (2003).

Standard locust saline containing (in mM): 147 NaCl, 10 KCl, 4 $CaCl_2$, 3 NaOH, and 10 HEPES buffer (pH 7.2) was perfused into the thoracic cavity through a glass pipette using a Peri-Star peristaltic pump (World Precision Instruments Inc., Sarasota, FL, USA). The saline flow was directed onto the MTG where the vCPG is located with overflow draining out of the posterior abdomen. The tissue covering the MTG was removed, followed by the cuticle and attached muscle tissue situated between the connectives, rostral to the metathoracic ganglion. A metal plate was placed beneath the MTG to stabilize it, and a silver wire was inserted into the caudal portion of the abdomen to ground the preparation.

2.4. Electromyographic recording of the motor pattern

An electromyographical (EMG) recording of the ventilatory motor pattern was obtained by resting the non-insulated tip of a 0.1 mm diameter insulated copper wire onto the ventilatory muscle 161 located in the second abdominal segment (A2). A DigiData 1200 Series Interface (Axon Instruments Inc., Union City, CA, USA) was used to digitize the ventilation recordings which were then displayed and recorded using AxoScope 9.0 software (Axon Instruments Inc.).

2.5. Extracellular potassium recording

K^+-sensitive and reference microelectrodes were connected to a pH/ion amplifier (Model 2000; A-M Systems Inc., Carlsborg, WA, USA). A K^+-sensitive and reference microelectrode pair was calibrated at room temperature (~21 °C) using 15 mM and 150 mM KCl solutions to obtain the voltage change, 'or slope', which was required for determination of $[K^+]_o$ (mM). A 10-fold change in $[K^+]$ resulted in a voltage change of ~58 mV and only electrode pairs with slope values very close to 58 mV (±4 mV) were accepted for experimental use. Following calibration, the K^+-sensitive and reference microelectrodes were inserted through the sheath of the MTG side-by-side in the region of the vCPG (Burrows, 1996). Specifically, the microelectrodes were placed centrally in the region of the first three abdominal neuromeres, which are fused to the metathoracic neuromere, forming the MTG. $[K^+]_o$ changes spread to other regions of the MTG (but not through the connectives), therefore placement of microelectrodes precisely at the vCPG was important to accurately measure the timing of $[K^+]_o$ disturbances surrounding the vCPG relative to arrest of the ventilatory motor pattern.

The $[K^+]_o$ was obtained by transforming the recorded $[K^+]_o$ trace in mV to mM using the Nernst equation:

$$E_K = \frac{RT}{zF} \ln \frac{[K^+]_o}{[K^+]_i}.$$

The following conversion of the above equation was used for determination of $[K^+]_o$ (mM):

$$[K^+]_o = 15 \times 10^{\text{voltage/slope}\,(\sim 58)}.$$

2.6. Pharmacological treatments

Drugs (Sigma–Aldrich) were dissolved in standard locust saline and bath-applied in semi-intact preparations as described above. Ouabain solutions were kept in opaque coverings to prevent exposure to light. All preparations were bathed in standard locust saline for a 10 min stabilization period prior to bath application of drugs. To examine the effects of different concentrations of ouabain 10^{-5} M, 10^{-4} M, and 10^{-3} M ouabain solutions were bath-applied in preparations for a minimum of 30 min. To examine the effects of potassium channel block 10^{-3} M TEA was bath-applied alone for 5 min followed by bath application of 10^{-3} M TEA in combination with 10^{-4} M ouabain for a minimum of 30 min.

The time to the initial $[K^+]_o$ event was calculated as the time from ouabain or TEA/ouabain application to the inflection point of the first abrupt increase in $[K^+]_o$. $[K^+]_o$ event duration was measured at half of the maximum amplitude and period was measured as the time from the upward inflection point of one $[K^+]_o$ event to the upward inflection point of the subsequent event. $[K^+]_o$ was calculated prior to the upward inflection point of the first surge as well as every 5 min thereafter to determine pre- as well as post-surge values. These values are termed "non-surge $[K^+]_o$". The closest non-surge $[K^+]_o$ was chosen if time points coincided with an $[K^+]_o$ event. The maximum $[K^+]_o$ peak value during $[K^+]_o$ events was also measured. $[K^+]_o$ event amplitudes were calculated by subtracting pre-surge $[K^+]_o$ from peak $[K^+]_o$. The change in extracellular $[K^+]$ during $[K^+]_o$ events is characterized by three distinct phases (Fig. 2D). The increase in $[K^+]_o$ from non-surge to peak values consists of one positive $[K^+]_o$ change referred to as the "up-slope". Once peak $[K^+]_o$ is reached there is a slow $[K^+]_o$ decrease referred to as the "top-slope". Finally, there is a switch from the slow top-slope phase to a steeper $[K^+]_o$ decrease termed the "down-slope". The up-, top-, and down-slopes for the first $[K^+]_o$ event were calculated at the point of greatest change during these phases. The probability of ventilatory motor pattern recovery following $[K^+]_o$ events was determined for preparations treated with 10^{-3} M and 10^{-4} M ouabain.

2.7. Statistical analyses

Data were plotted using SigmaPlot 9.0 (SPSS Inc., Chicago, IL, USA) and presented as the mean and standard error (S.E.). Statistical analyses were performed using SigmaStat 3.0 statistical analysis software (SPSS Inc.). *t*-Tests were used to determine if there were statistically significant differences in overall means between treatment groups (10^{-4} M vs. 10^{-3} M ouabain and 10^{-4} M ouabain alone vs. 10^{-4} M ouabain in combination with 10^{-3} M TEA). Two-way repeated measure (RM) ANOVAs were used to determine if there were statistically significant differences in mean measurements repeatedly taken over the duration of experiments between treatment groups. A two-way ANOVA was used to determine if there were significantly different mean slopes of $[K^+]_o$ increase and decrease during the first $[K^+]_o$ surge between treatment groups (two subject factors: 10^{-4} M vs. 10^{-3} M ouabain and up-, top-, or down-slope). *Post hoc* Tukey tests were performed to determine which groups drove the main effects. A Kaplan–Meier Survival Analysis was conducted in order to determine if there were significant differences in the ability of the vCPG to recover following $[K^+]_o$ surges induced by 10^{-4} M vs. 10^{-3} M ouabain. A *z*-test was used to compare the proportion of preparations treated with 10^{-4} M ouabain alone vs. 10^{-4} M ouabain in combination with 10^{-3} M TEA that had at least one $[K^+]_o$ event. A 95% confidence interval was used to determine significance.

3. Results

3.1. Ouabain-induced inhibition of the Na^+/K^+-ATPase elicits repetitive $[K^+]_o$ events

Ventilatory motor pattern activity and extracellular potassium ion concentration surrounding the vCPG were measured during treatment with different doses of the Na^+/K^+-ATPase inhibitor ouabain (Fig. 1). It was shown previously that continuous bath application of 10^{-4} M ouabain elicits multiple surges in $[K^+]_o$ where the rise and fall of $[K^+]_o$ are associated with arrest and recovery of the vCPG, respectively (Rodgers et al., 2007). It was of interest to further explore this phenomenon and characterize the concentration-dependence of the effect of ouabain. A relationship between repetitive $[K^+]_o$ surges in the locust MTG and the concentration of ouabain in the bathing saline would indicate the level of inhibition of Na^+/K^+ transporters and thus the rate of clearance of $[K^+]_o$ plays a role in vCPG arrest and the associated $[K^+]_o$ surge. We found that continuous bath application of two different concentrations of ouabain, 10^{-4} M and 10^{-3} M, elicited multiple abrupt surges in $[K^+]_o$ (Fig. 1A and B). 10^{-5} M ouabain was bath-applied in a total of four preparations and induced a single $[K^+]_o$ event in only one of these preparations (data not shown). During 10^{-4} M ouabain application the arrest and recovery of the ventilatory motor pattern were associated with the rise and fall of $[K^+]_o$, respectively (Fig. 1A). $[K^+]_o$ clearance always coincided with recovery of motor pattern generation, however the ventilatory rhythm frequency and duration became more variable following each $[K^+]_o$ surge (Fig. 1A). During 10^{-3} M ouabain application complete loss of the ventilatory motor pattern was eventually seen (Fig. 1B). $[K^+]_o$ events were reliably induced during both 10^{-4} M ($N = 8$) and 10^{-3} M ($N = 9$) ouabain treatment, with 100% of preparations ($N_{total} = 17$) having at least one $[K^+]_o$ event, however preparations treated with 10^{-3} M ouabain had a significantly greater number of $[K^+]_o$ events (*t*-test, $t = -2.955$, $P = 0.010$, d.f. = 15) (Fig. 1C).

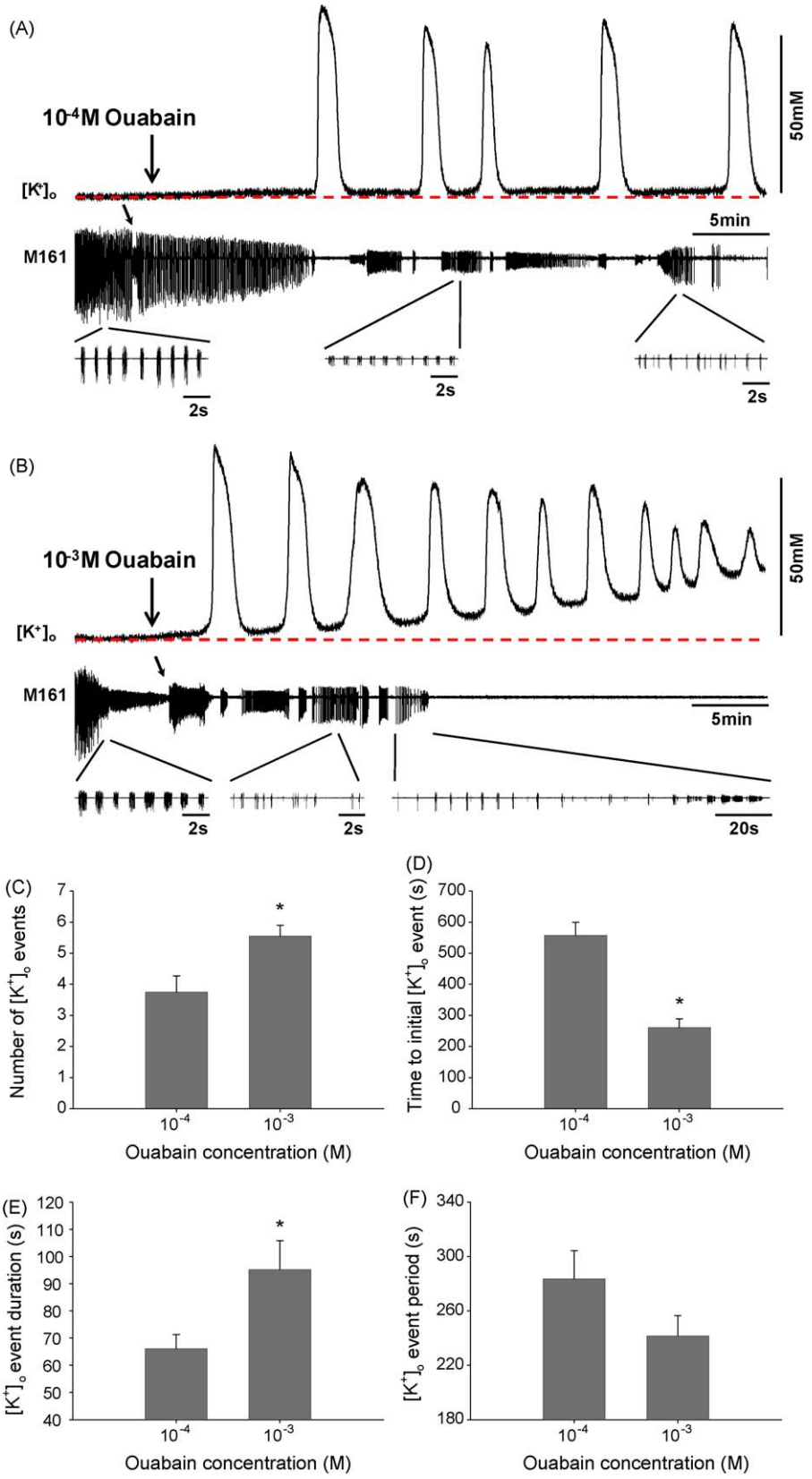

Fig. 1. Simultaneous recordings of electrical activity from muscle 161 (M161) in the second abdominal segment and the extracellular potassium concentration ($[K^+]_o$) surrounding the vCPG. Continuous bath application of both 10^{-4} M ($N = 8$) and 10^{-3} M ($N = 9$) ouabain induced multiple all-or-none increases in $[K^+]_o$. (A) During 10^{-4} M ouabain treatment each $[K^+]_o$ event was associated with arrest of the ventilatory motor pattern and a period of depression of electrical activity from M161. Recovery of motor pattern generation was associated with return of $[K^+]_o$ to near pre-surge levels. (B) During 10^{-3} M ouabain treatment non-surge $[K^+]_o$ levels progressively increased. An inability to recover motor pattern generation was common during 10^{-3} M ouabain treatment. (A and B) There was often a burst of unpatterned electrical activity following arrest of the ventilatory motor pattern during $[K^+]_o$ events. Expanded regions of EMG recordings from ventilatory muscle 161 show increased variability of the motor pattern following multiple $[K^+]_o$ events. Diagonal arrows above M161 recordings indicate anomalies in the motor pattern due to readjustment of the EMG electrode. (C) All

3.2. Timing of repetitive $[K^+]_o$ events during 10^{-4} M and 10^{-3} M ouabain treatment

We examined various parameters related to the timing of $[K^+]_o$ events induced by 10^{-4} M and 10^{-3} M ouabain. Latency to onset of ouabain-induced $[K^+]_o$ surging was measured to determine how the degree of Na^+/K^+-ATPase inhibition by ouabain affects initiation of repetitive $[K^+]_o$ events, if at all. The time from ouabain application to the initial $[K^+]_o$ event was significantly shorter in preparations treated with 10^{-3} M ouabain compared to 10^{-4} M ouabain (*t*-test, $t = -5.949$, $P < 0.001$, d.f. = 15) (Fig. 1D). Duration, measured at half the maximum amplitude of each $[K^+]_o$ event, was analyzed in preparations treated with 10^{-4} M and 10^{-3} M ouabain to characterize the difference in the ability of neuronal tissue to recover from the $[K^+]_o$ disturbance. There was a main effect of ouabain concentration on the duration of the first five $[K^+]_o$ events (two-way RM-ANOVA, $P = 0.008$, $F_{(1,19)} = 14.620$), however $[K^+]_o$ event duration did not change over time (two-way RM-ANOVA, $P = 0.181$, $F_{(4,19)} = 1.699$) (data not shown). The mean duration at half the maximum amplitude of the first $[K^+]_o$ event was significantly longer in preparations treated with 10^{-3} M ouabain compared to those treated with 10^{-4} M ouabain (*t*-test, $t = -2.352$, $P = 0.033$, d.f. = 15) (Fig. 1E). $[K^+]_o$ event period, i.e. the time from the upward inflection point of one surge to the upward inflection point of the next surge, was measured to determine if a higher concentration of ouabain increased the frequency of respective $[K^+]_o$ events. There was no main effect of ouabain concentration on the period of the first five $[K^+]_o$ events (two-way RM-ANOVA, $P = 0.705$, $F_{(1,18)} = 0.157$) and $[K^+]_o$ event period did not change over time (two-way RM-ANOVA, $P = 0.222$, $F_{(4,18)} = 1.529$) (data not shown). There was no significant difference between the two concentrations in the mean period from the first to the second $[K^+]_o$ event (*t*-test, $t = 1.691$, $P = 0.111$, d.f. = 15) (Fig. 1F). These results show that there is a shorter latency between the first two $[K^+]_o$ events elicited during 10^{-3} M ouabain application compared to during 10^{-4} M ouabain application.

3.3. Characteristics of $[K^+]_o$ surrounding the vCPG during 10^{-4} M and 10^{-3} M ouabain treatment

We measured non-surge $[K^+]_o$ prior to the initial $[K^+]_o$ event and every 5 min thereafter in order to determine if the degree of pump inhibition affects the ability to recover $[K^+]_o$ to initial levels over the 30 min duration of ouabain application. There was a main effect of ouabain concentration on pre- and post-surge $[K^+]_o$ during a 30 min bath application (two-way RM-ANOVA, $P < 0.001$, $F_{(1,24)} = 33.179$) (Fig. 2A). Preparations treated with 10^{-3} M ouabain had significantly higher non-surge $[K^+]_o$ levels measured at 25 and 30 min following initial ouabain application compared to preparations treated with 10^{-4} M ouabain (*post hoc* Tukey tests, $P < 0.05$) (Fig. 2A). In addition, the non-surge $[K^+]_o$ in preparations treated with 10^{-4} M and 10^{-3} M ouabain responded differently to increased time of exposure (significant interaction between ouabain concentration and time: two-way RM-ANOVA, $P = 0.003$, $F_{(6,24)} = 4.560$) (Fig. 2A). There was a main effect of ouabain concentration on the peak $[K^+]_o$ of the first five $[K^+]_o$ events (two-way RM-ANOVA, $P = 0.003$, $F_{(1,23)} = 5.019$), however peak $[K^+]_o$ did not change over time (two-way RM-ANOVA, $P = 0.134$, $F_{(4,23)} = 2.863$) (data not shown). The average peak $[K^+]_o$, calculated from the peak values of the first $[K^+]_o$ event, was significantly lower in preparations treated with 10^{-3} M ouabain compared to 10^{-4} M ouabain (*t*-test, $t = 2.292$, $P = 0.037$, d.f. = 15) (Fig. 2B). There was a main effect of ouabain concentration on the amplitude of $[K^+]_o$ increase during the first five $[K^+]_o$ events (two-way RM-ANOVA, $P < 0.001$, $F_{(1,23)} = 6.960$), however amplitude of $[K^+]_o$ events did not change over time (two-way ANOVA, $P = 0.073$, $F_{(1,23)} = 4.396$) (data not shown). The mean amplitude of the $[K^+]_o$ increase of the first $[K^+]_o$ event was significantly lower in preparations treated with 10^{-3} M ouabain compared to 10^{-4} M ouabain (*t*-test, $t = 2.319$, $P < 0.035$, d.f. = 15) (Fig. 2C). There was no main effect of ouabain concentration on the slopes of the $[K^+]_o$ increase and decrease of the first $[K^+]_o$ event elicited by 10^{-4} M and 10^{-3} M ouabain treatment (two-way ANOVA, $P = 0.813$, $F_{(1,45)} = 0.0565$), however there was a significant interaction between ouabain concentration and the location of slopes (two-way ANOVA, $P = 0.008$, $F_{(2,45)} = 5.456$) (Fig. 2D). The up-slopes of the first surges elicited during 10^{-4} M and 10^{-3} M ouabain application were significantly different (*post hoc* Tukey test, $P < 0.05$) (Fig. 2D). A trend occurred during the downward phase of every first $[K^+]_o$ event, as two seemingly different slopes were present. The rate of $[K^+]_o$ decrease was significantly smaller during the top-slope phase compared to the down-slope phase and this difference occurred irrespective of ouabain concentration (*post hoc* Tukey tests, $P < 0.05$) (Fig. 2D). When examining top-slopes and down-slopes individually, there was no effect of ouabain concentration on the magnitude of these slopes (*post hoc* Tukey tests, $P > 0.05$) (Fig. 2D).

3.4. Arrest and recovery of the ventilatory motor pattern

All preparations had a robust ventilatory motor pattern during the initial stages of both 10^{-3} M and 10^{-4} M ouabain application. As time of exposure to ouabain increased and following each $[K^+]_o$ event there was a concentration-dependent difference in the ability of preparations to recover generation of a motor pattern (data not shown). Overall the probability of motor pattern recovery following $[K^+]_o$ events during 10^{-3} M ouabain application was significantly lower than during 10^{-4} M ouabain application (Kaplan–Meier Survival Analysis, Gehan–Breslow test statistic = 12.077, $P < 0.001$, d.f. = 1). In one preparation treated with 10^{-3} M ouabain motor pattern recovery did not occur following the first $[K^+]_o$ event or subsequent $[K^+]_o$ events. The motor pattern did not recover following the fourth $[K^+]_o$ event in any preparation treated with 10^{-3} M ouabain. During 10^{-3} M ouabain treatment, the average time to complete ventilatory motor pattern failure was 10.4 ± 1.3 min from initial ouabain application. During 10^{-4} M ouabain application only one preparation exhibited complete ventilatory motor pattern failure which occurred following the fourth $[K^+]_o$ event.

3.5. Effect of potassium channel block on ouabain-induced repetitive ventilatory arrest

10^{-3} M TEA, a nonselective voltage-gated K^+ channel inhibitor, was bath-applied in combination with 10^{-4} M ouabain in order to determine if ouabain-induced $[K^+]_o$ events are modulated by K^+

preparations treated with ouabain generated repetitive $[K^+]_o$ events, but a significantly greater number of $[K^+]_o$ events were elicited by 10^{-3} M ouabain compared to 10^{-4} M ouabain. (D) Time to onset of the initial $[K^+]_o$ event (s) in response to 10^{-4} M ($N = 8$) and 10^{-3} M ($N = 9$) ouabain bath application. 10^{-3} M ouabain hastened the onset of the first $[K^+]_o$ event in comparison to 10^{-4} M ouabain. (E) Mean duration (s) of the first $[K^+]_o$ event during 10^{-3} M ($N = 9$) ouabain application was significantly longer than during 10^{-4} M ($N = 8$) ouabain application. $[K^+]_o$ event durations were calculated using the duration at half the maximum amplitude of each $[K^+]_o$ event. (F) There was no significant difference in the period (s) from the first to the second $[K^+]_o$ event during 10^{-4} M ($N = 8$) and 10^{-3} M ($N = 9$) ouabain application. $[K^+]_o$ event periods were calculated as the time from the inflection point of the $[K^+]_o$ increase of the first event to the inflection point of the $[K^+]_o$ increase of the second event. Data are means ± S.E. and the asterisks indicate significant differences between 10^{-4} M and 10^{-3} M ouabain treatments.

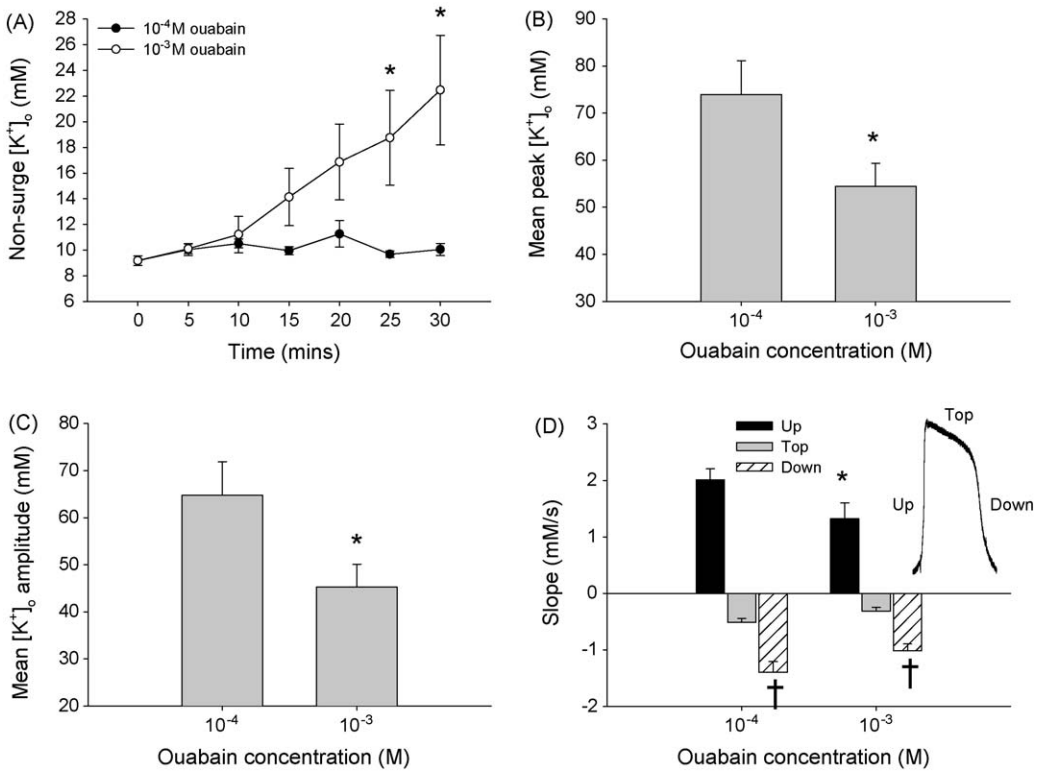

Fig. 2. (A) Mean non-surge $[K^+]_o$ levels (mM) during continuous bath application of 10^{-4} M and 10^{-3} M ouabain. Non-surge $[K^+]_o$ was measured prior to the first $[K^+]_o$ event (time = 0) and every 5 min thereafter (where possible). $[K^+]_o$ returned to initial levels following each $[K^+]_o$ event during 10^{-4} M ouabain application, whereas non-surge $[K^+]_o$ progressively increased during treatment with 10^{-3} M ouabain. (B) Mean peak $[K^+]_o$ (mM) of the first $[K^+]_o$ event during 10^{-4} M and 10^{-3} M ouabain bath application. Peak $[K^+]_o$ of the first $[K^+]_o$ event elicited by 10^{-3} M ($N = 9$) ouabain treatment was significantly decreased compared to peak values in preparations treated with 10^{-4} M ($N = 8$) ouabain. (C) The amplitude of $[K^+]_o$ increase (mM) was calculated as the difference between the peak $[K^+]_o$ during an $[K^+]_o$ event and the preceding non-surge $[K^+]_o$. The mean amplitude $[K^+]_o$ of the first $[K^+]_o$ event during 10^{-3} M ($N = 9$) ouabain application was significantly lower compared to the amplitude of the first $[K^+]_o$ event elicited by 10^{-4} M ($N = 8$) ouabain application. (D) Three distinct slopes could be detected during $[K^+]_o$ events, as displayed in the inset: "Up" slope from pre-surge to maximum peak $[K^+]_o$, "Top" slope from maximum peak $[K^+]_o$ to the first downward inflection point, and "Down" slope from the first downward inflection point to post-surge $[K^+]_o$. Up-slopes generated by 10^{-4} M and 10^{-3} M ouabain were significantly different, however ouabain concentration did not have an effect on top- and down-slopes. Top- and down-slopes were significantly different irrespective of ouabain dose (indicated by daggers). Sample sizes (10^{-4} M, 10^{-3} M): $N_{Up} = 8.9$; $N_{Top} = 8.9$; $N_{Down} = 8.9$. Data are means ± S.E. and the asterisks indicate significant differences between 10^{-4} M and 10^{-3} M ouabain treatments.

conductances (Fig. 3A). Bath application of 10^{-3} M TEA in combination with 10^{-4} M ouabain ("OUA/TEA") significantly reduced the likelihood of producing ouabain-induced $[K^+]_o$ events compared to preparations treated with 10^{-4} M ouabain alone ("OUA"; Fig. 1A) (z-test, $z = 2.028$, $P = 0.043$) (Fig. 3B). The proportions of OUA and OUA/TEA preparations that had at least one $[K^+]_o$ event were 1 (8/8) and 0.6 (6/10), respectively (Fig. 3B). Of the preparations that had at least one $[K^+]_o$ event, TEA treatment significantly reduced the number of events (t-test, $t = 3.079$, $P = 0.010$, d.f. = 12) (Fig. 3C). In addition, TEA significantly increased the time to onset of ouabain-induced $[K^+]_o$ events (t-test, $t = -2.555$, $P = 0.025$, d.f. = 12) (Fig. 3D), and K^+ channel block significantly reduced the absolute value of $[K^+]_o$ increases during the first three $[K^+]_o$ events compared to preparations treated with ouabain alone (two-way RM-ANOVA, $P = 0.001$, $F_{(1,7)} = 23.659$) (Fig. 3E).

4. Discussion

We found that ouabain-induced Na^+/K^+-ATPase inhibition elicits repetitive arrest of ventilatory motor pattern generation in the locust. Each period of electrical activity depression occurred simultaneously with abrupt increases in $[K^+]_o$, where the rise and fall of $[K^+]_o$ coincided with arrest and recovery of the ventilatory motor pattern, respectively. It is intriguing that Na^+/K^+-ATPase dysfunction induced repetitive waves of $[K^+]_o$ increase and decrease as opposed to a gradual increase in $[K^+]_o$. $[K^+]_o$ remained fairly stable during the time from initial ouabain bath application to the initial abrupt increase in $[K^+]_o$, indicating that there is a threshold for the $[K^+]_o$ disturbance. The Na^+/K^+-ATPase is under the control of a wide range of regulatory mechanisms and pathways and can be regulated by changes in ions such as Na^+ (Kaplan, 2002). Pump inhibition causes an increase in the intracellular sodium concentration ($[Na^+]_i$) which in turn stimulates Na^+/K^+-ATPase complexes free of ouabain block to work more rapidly to expel the excess Na^+ (Kaplan, 2002). We suggest that the threshold for the abrupt $[K^+]_o$ increase occurs at a point when functioning Na^+/K^+ pumps fail to cope with changing concentration gradients as a result of ouabain. At this point the system enters a positive feedback cycle in which increasing $[K^+]_o$ causes cellular depolarization that opens voltage-dependent channels and the flux of K^+ ions into the extracellular space. Our model for ouabain-induced cyclic K^+ increases is depicted in Fig. 4. We hypothesize that spreading depression (SD)-like events in the locust (Rodgers et al., 2007) are triggered by positive feedback processes involving an initial ionic disturbance reaching a threshold and caused by neuronal overexcitation or by treatments or conditions that impair ionic homeostasis (Grafstein, 1956; van Harreveld, 1978; Balestrino et al., 1999; Somjen, 2001). We believe that the positive feedback cycle is initiated when processes of $[K^+]_o$ accumulation overwhelm the ability to clear $[K^+]_o$ from a restricted interstitium with limited glial buffering capacity (Somjen and Müller, 2000; Kager et al., 2000, 2002; Somjen, 2002), changing the equilibrium potential for K^+ and depolarizing membranes. The conductances

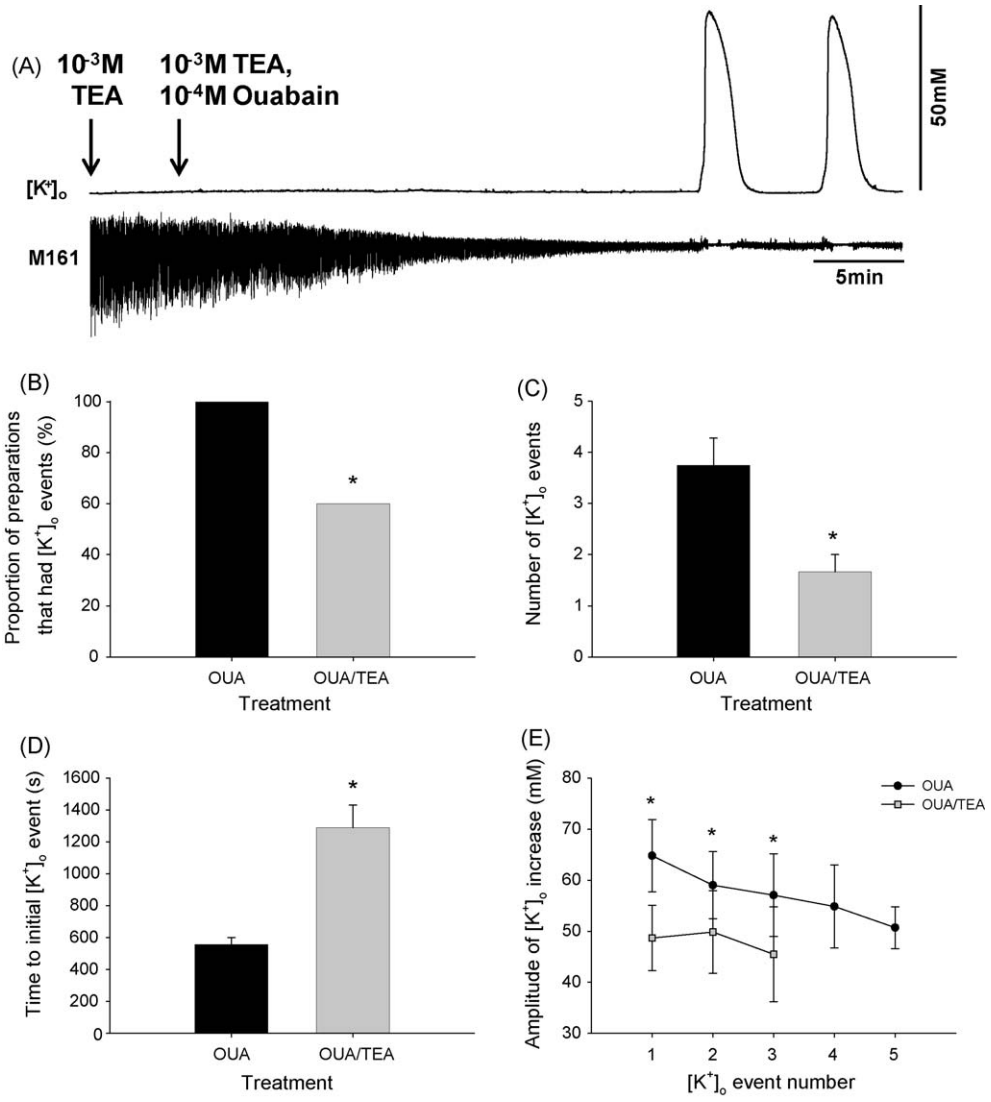

Fig. 3. (A) Simultaneous recording of electrical activity from muscle 161 (M161) and the extracellular potassium concentration ($[K^+]_o$) surrounding the vCPG. 10^{-3} M TEA was bath-applied for 5 min alone, then in combination with 10^{-4} M ouabain for 40 min. In the experiment shown here 10^{-3} M TEA delayed the onset of ouabain-induced $[K^+]_o$ events, thereby reducing the number of events that occurred compared to preparations treated with 10^{-4} M ouabain alone. Note that reduction in amplitude of the EMG recording is attributable to the effect of TEA at the neuromuscular junction. (B–D) Preparations treated with 10^{-4} M ouabain alone are termed "OUA" (Fig. 1A) and preparations treated with 10^{-3} M TEA in combination with 10^{-4} M ouabain are termed "OUA/TEA". (B) Block of voltage-gated potassium channels with TEA significantly reduced the proportion of preparations that had at least one $[K^+]_o$ event ($N_{OUA} = 8$; $N_{OUA/TEA} = 10$). (C) TEA reduced the severity of ouabain-induced $[K^+]_o$ events by significantly decreasing the number of $[K^+]_o$ events ($N_{OUA} = 8$; $N_{OUA/TEA} = 6$). (D) The time from initial ouabain application to the initial $[K^+]_o$ event was increased in preparations that had simultaneous TEA treatment ($N_{OUA} = 8$; $N_{OUA/TEA} = 6$). (E) The amplitude of $[K^+]_o$ events in preparations treated with TEA was reduced compared to preparations treated with ouabain alone ($N_{OUA} = 8$; $N_{OUA/TEA} = 6$). Data are means ± S.E. and the asterisks indicate significant differences between OUA and OUA/TEA treatments.

involved in the repetitive $[K^+]_o$ events in the locust are not known, but could be due to opening of voltage-dependent or ATP-sensitive K^+ channels of neurons or glia. Nonselective conductances could also explain the intense outflow of K^+. In vertebrate pyramidal neurons pannexin 1 (Px1) hemichannels, or half gap junctions, open during ischemic-like conditions (oxygen/glucose deprivation) (Thompson et al., 2006). Interestingly, invertebrate neuronal gap junctions are composed of Px1 proteins (Panchin, 2005), and these nonselective cation channels could be a conduit of K^+ efflux during ouabain-induced repetitive $[K^+]_o$ events in the locust. The mechanisms underlying the repetitive nature of ouabain-induced $[K^+]_o$ events remain to be precisely defined, however we suggest that when activity ceases as a result of a $[K^+]_o$ event, the remaining K^+ clearance mechanisms are sufficient to cause the system to enter another positive feedback cycle whereby decreasing $[K^+]_o$ causes membrane hyperpolarization that closes voltage-dependent K^+ channels and reduces the flux of K^+ across the membrane (Fig. 4). Our results demonstrate that the balance of $[K^+]_o$ accumulation and clearance is biased by the degree of Na^+/K^+-ATPase inhibition by ouabain.

Consistent with this model 10^{-3} M ouabain bath application hastened the time to onset of the initial $[K^+]_o$ event and elicited a greater number of $[K^+]_o$ events compared to 10^{-4} M ouabain treatment. Following initial ouabain application it took approximately 4 min (261 ± 27 s) for 10^{-3} M ouabain to generate the initial $[K^+]_o$ event compared to approximately 9 min (557 ± 43 s) in response to 10^{-4} M ouabain application. Differences in latency to onset suggest that the threshold for the initial $[K^+]_o$ disturbance is dependent on the degree of Na^+/K^+-ATPase saturation by ouabain. Duration, measured at half the maximum amplitude of each $[K^+]_o$ event, was analyzed to determine how fast the neuronal tissue was able to recover from the $[K^+]_o$ disturbance. We found that the $[K^+]_o$

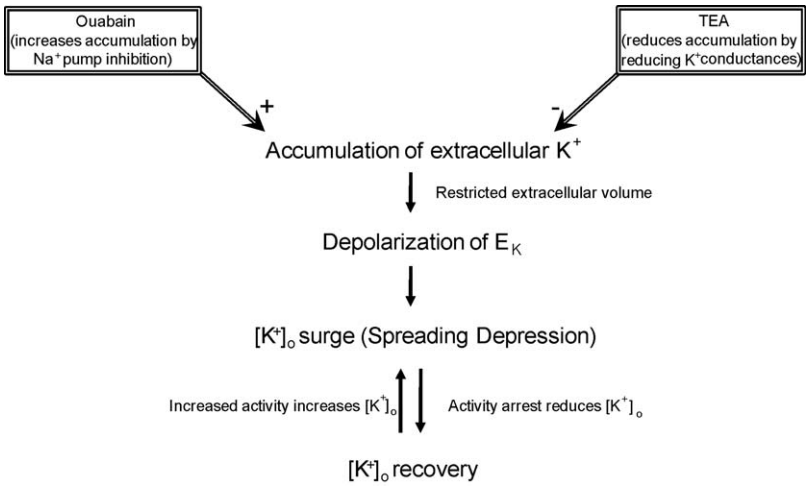

Fig. 4. A model describing a possible mechanism for the abrupt $[K^+]_o$ increase and subsequent $[K^+]_o$ recovery in response to cellular stressors in the locust metathoracic ganglion. $[K^+]_o$ accumulation surrounding the vCPG occurs due to impaired clearance mechanisms (Na^+K^+-ATPase dysfunction using ouabain) or increased neuronal activity in an extracellular compartment with small volume. With low concentrations of ouabain or low activity levels pump regulation can accommodate the change in $[K^+]_o$ and maintain concentration gradients (e.g. 10^{-5} M ouabain). High concentrations of ouabain impair $[K^+]_o$ clearance sufficiently to change the equilibrium potential for K^+ and depolarize membranes. Depolarization of E_K initiates a positive feedback cycle where depolarization leads to opening of voltage-dependent channels, increased activity, further increases in $[K^+]_o$, leading again to further depolarization. At the peak of the $[K^+]_o$ surge activity ceases due to inactivation of Na^+ channels, allowing remaining $[K^+]_o$ clearance mechanisms to counteract $[K^+]_o$ accumulation. This process leads into another positive feedback cycle at the point at which restoration of the ion gradient begins to hyperpolarize membranes, which in turn closes voltage-dependent K^+ channels and reduces the process of $[K^+]_o$ accumulation. Thus, the repetitive nature of $[K^+]_o$ surges induced by 10^{-4} M ouabain depends on the balance of $[K^+]_o$ clearance and accumulation.

event durations during 10^{-3} M ouabain application were significantly longer than during 10^{-4} M ouabain application. If blocking more Na^+/K^+-ATPase pumps using a higher concentration of ouabain (10^{-3} M) causes longer duration $[K^+]_o$ events, then it could be suggested that Na^+/K^+-ATPase transporters play a key role in recovery from this state of homeostatic disruption (Leis et al., 2005). Analysis of the $[K^+]_o$ event period revealed no significant difference between 10^{-4} M and 10^{-3} M ouabain treatments. Thus duration and period data demonstrate that there is a shorter latency between $[K^+]_o$ events elicited during 10^{-3} M ouabain application compared to during 10^{-4} M ouabain application.

During 10^{-4} M ouabain application non-surge extracellular $[K^+]$ levels remained relatively stable, with $[K^+]_o$ returning to near initial levels following each abrupt increase. Application of 10^{-3} M ouabain resulted in a gradual increase in non-surge $[K^+]_o$ following each $[K^+]_o$ event until the mean $[K^+]_o$ at 25 min and 30 min of treatment was significantly higher than the corresponding 10^{-4} M value. In the dentate gyrus of adult rat hippocampal slices application of a relatively high concentration of ouabain prevents the return of $[K^+]_o$ to baseline levels following a surge (Xiong and Stringer, 2000). We suggest that the gradual rise in $[K^+]_o$ during 10^{-3} M ouabain application is indicative of Na^+/K^+ pumps becoming progressively inhibited as more become blocked, causing $[K^+]_o$ to accumulate.

If $[K^+]_o$ clearance mechanisms are impaired, then it would be logical to assume that the rate of $[K^+]_o$ clearance, or down-slope, during $[K^+]_o$ events would be negatively affected (McCarren and Alger, 1987; Xiong and Stringer, 2000). The up-slopes of the first $[K^+]_o$ event during 10^{-4} M and 10^{-3} M ouabain treatment were significantly different, however there was no significant difference in the down-slopes associated with motor pattern recovery. An interesting characteristic of the initial $[K^+]_o$ event is the two seemingly different slopes during the return of $[K^+]_o$ to baseline values. Although there was no significant difference between the top- or down-slopes of the first $[K^+]_o$ event across ouabain concentrations, the top- and down-slopes were significantly different irrespective of ouabain dose which indicates an abrupt change in $[K^+]_o$ clearance mechanisms. Following an abrupt increase in $[K^+]_o$ and arrest of the ventilatory motor pattern $[K^+]_o$ accumulation will necessarily decrease once neural activity has ceased allowing remaining mechanisms of clearance to predominate until the threshold for rapid recovery is reached. The change in the trajectory of recovery may simply reflect the accelerating nature of a positive feedback mechanism.

In addition to Na^+/K^+-ATPase impairment other cellular stressors, including hyperthermia, ATP depletion, and anoxia, cause arrest of the ventilatory motor pattern that is associated with abrupt all-or-none type increases in $[K^+]_o$ in the vCPG region of the MTG (Rodgers et al., 2007). These stress-induced $[K^+]_o$ events share many characteristics with cortical spreading depression (CSD), characterized as a massive redistribution of ions, notably $[K^+]_o$ and $[Na^+]_i$, accompanied by a rapid and nearly complete depolarization of neurons in vertebrate cortical tissue (Leao, 1944; Hansen and Zeuthen, 1981; Gorji, 2001; Somjen, 2001). What is quite intriguing is that the ionic changes during SD trigger surrounding neuronal cells to follow suit (Hansen and Zeuthen, 1981; Somjen, 2001). The end result is a depression of neural activity that arises from a focal point, and spreads throughout the cerebral cortex at a rate of approximately 2–5 mm/min (Leao, 1944). SD events propagate within the locust MTG at a rate similar to that in cortical tissue (2.4 ± 0.04 mm/min) (Rodgers et al., 2007) and the ouabain-induced repetitive SD-like events in our study could represent propagating waves of $[K^+]_o$ increase and decrease passing by the K^+-sensitive electrode tip. We suggest that arrest of the vCPG coincides with an abrupt $[K^+]_o$ increase surrounding the CPG that spreads locally to other regions of the neuropil via diffusion across the extracellular space and possibly through gap junctions. Given that $[K^+]_o$ events spread within the locust MTG at a rate of ~2 mm/min we conclude that the entire ganglion is affected during the ~1 min duration of $[K^+]_o$ events. Several studies have exploited the ability of ouabain in blocking the Na^+/K^+-ATPase in order to study SD in mammalian brain tissue (Haglund and Schwartzkroin, 1990; Balestrino et al., 1999; Menna et al., 2000; Xiong and Stringer, 2000). It is possible that Na^+/K^+-ATPase inhibition is primarily responsible for the neural circuitry impairment that occurs in response to cellular stressors in the locust.

We found that block of voltage-gated K^+ channels with TEA suppressed ouabain-induced repetitive ventilatory arrest and the associated $[K^+]_o$ events. TEA blocks voltage-gated K^+ channels in a nonselective manner and it is not known which subtypes of K^+ channels are blocked by TEA at a given concentration in the locust CNS. It has been shown that TEA diminishes the amplitude of hyperthermia-induced $[K^+]_o$ events in the locust (Rodgers et al., 2007), suggesting that at least part of the K^+ leaving cells during the abrupt stress-induced $[K^+]_o$ increase flows through TEA-sensitive channels (Somjen, 2001). TEA also diminished the amplitude $[K^+]_o$ of ouabain-induced $[K^+]_o$ events compared to preparations treated with 10^{-4} M ouabain alone. TEA both reduced neuronal K^+ release and prolonged the circling time of self-sustaining circling SD in the chicken retina (RSD) (Scheller et al., 1998). Scheller et al. (1998) concluded that TEA reduced the RSD-mediated neuronal K^+ release, thereby reducing K^+ re-uptake and buffering by glial cells, which resulted in decreased re-initiation of RSD and consequently decreased propagation velocity. We suggest that the TEA-induced reduction of K^+ conductances in our study resulted in reduced $[K^+]_o$ clearance requirements of un-inhibited Na^+/K^+ pumps, allowing these pumps to better maintain K^+ homeostasis (Fig. 4).

In conclusion we show that ouabain-induced Na^+/K^+-ATPase dysfunction elicits repetitive SD-like events that are concentration-dependent. In addition, we provide evidence for a role for K^+ channels in modulation of ouabain-induced repetitive SD-like events in the locust CNS. We propose that our manipulations acted on either side of a balance between processes of accumulation and clearance of extracellular $[K^+]$ and that ventilatory arrest occurs when the balance is such that $[K^+]_o$ is able to accumulate sufficiently to change the potassium equilibrium potential and cause cellular depolarization.

Acknowledgment

We thank the Natural Sciences and Engineering Research Council of Canada for funding.

References

Balestrino, M., Young, J., Aitken, P., 1999. Block of (Na^+, K^+) ATPase with ouabain induces spreading depression-like depolarization in hippocampal slices. Brain Research 838 (1–2), 37–44.

Burrows, M., 1996. The Neurobiology of an Insect Brain. Oxford University Press, Oxford.

Bustami, H.P., Hustert, R., 2000. Typical ventilatory pattern of the intact locust is produced by the isolated CNS. Journal of Insect Physiology 46 (9), 1285–1293.

Erecinska, M., Silver, I.A., 1994. Ions and energy in mammalian brain. Progress in Neurobiology 43 (1), 37–71.

Erulkar, S.D., Weight, F.F., 1977. Extracellular potassium and transmitter release at the giant synapse of squid. Journal of Physiology 266 (2), 209–218.

Gorji, A., 2001. Spreading depression: a review of the clinical relevance. Brain Research Reviews 38 (1–2), 33–60.

Grafstein, B., 1956. Mechanism of spreading cortical depression. Journal of Neurophysiology 19 (2), 154–171.

Haglund, M.M., Schwartzkroin, P.A., 1990. Role of Na–K pump potassium regulation and IPSPs in seizures and spreading depression in immature rabbit hippocampal slices. Journal of Neurophysiology 63 (2), 225–239.

Hansen, A.J., Zeuthen, T., 1981. Extracellular ion concentrations during spreading depression and ischemia in the rat brain cortex. Acta Physiologica Scandinavica 113 (4), 437–445.

Harrison, J.F., 1997. Ventilatory mechanism and control in grasshoppers. American Zoologist 37 (1), 73–81.

Huxley, A.F., Stämpfli, R., 1951. Effect of potassium and sodium on resting and action potentials of single myelinated nerve fibers. Journal of Physiology 112 (3–4), 496–508.

Kager, H., Wadman, W.J., Somjen, G.G., 2000. Simulated seizures and spreading depression in a neuron model incorporating interstitial space and ion concentrations. Journal of Neurophysiology 84 (1), 495–512.

Kager, H., Wadman, W.J., Somjen, G.G., 2002. Conditions for the triggering of spreading depression studies with computer simulations. Journal of Neurophysiology 88 (5), 2700–2712.

Kaplan, J.H., 2002. Biochemistry of Na K-ATPase. Annual Review of Biochemistry 71, 511–535.

Kretzschmar, D., Pflugfelder, G.O., 2002. Glia in development, function, and neurodegeneration of the adult insect brain. Brain Research Bulletin 57 (1), 121–131.

Leao, A.A.P., 1944. Spreading depression of activity in the cerebral cortex. Journal of Neurophysiology 7 (6), 359–390.

Leis, J.A., Bekar, L.K., Walz, W., 2005. Potassium homeostasis in the ischemic brain. Glia 50 (4), 407–416.

McCarren, M., Alger, B.E., 1987. Sodium-potassium pump inhibitors increase neuronal excitability in the rat hippocampal slice: role of a Ca^{2+}-dependent conductance. Journal of Neurophysiology 57 (2), 496–509.

Menna, G., Tong, C.K., Chesler, M., 2000. Extracellular pH changes and accompanying cation shifts during ouabain-induced spreading depression. Journal of Neurophysiology 83 (3), 1338–1345.

Newman, A.E.M., Foerster, M., Shoemaker, K.L., Robertson, R.M., 2003. Stress-induced thermotolerance of ventilatory motor pattern generation in the locust, *Locusta migratoria*. Journal of Insect Physiology 49 (11), 1039–1047.

Newman, E.A., 1993. Inward-rectifying potassium channels in retinal glial (Müller) cells. Journal of Neuroscience 13 (8), 3333–3345.

Orkand, R.K., Nicholls, J.G., Kuffler, S.W., 1966. Effect of nerve impulses on the membrane potential of glial cells in the central nervous system of amphibian. Journal of Neurophysiology 29 (4), 788–806.

Panchin, Y.V., 2005. Evolution of gap junction proteins—the pannexin alternative. Journal of Experimental Biology 208 (8), 1415–1419.

Ramirez, J.M., Pearson, K.G., 1989. Distribution of intersegmental interneurons that can reset the respiratory rhythm of the locust. Journal of Experimental Biology 141 (1), 151–176.

Robertson, R.M., 2004. Thermal stress and neural function: adaptive mechanisms in insect model systems. Journal of Thermal Biology 29 (7–8), 351–358.

Rodgers, C.I., Armstrong, G.A.B., Shoemaker, K.L., LaBrie, J.D., Moyes, C.D., Robertson, R.M., 2007. Stress preconditioning of spreading depression in the locust CNS. PLoS ONE 2, e1366, doi:10.1371/journal.pone.0001366.

Rounds, H.D., 1967. KCl-induced 'spreading depression' in the cockroach. Journal of Insect Physiology 13, 869–872.

Scheller, D., Tegtmeier, F., Schule, W.-R., 1998. Dose-dependent effects of tetraethylammonium on circling spreading depressions in chicken retina. Journal of Neuroscience Research 51 (1), 85–89.

Somjen, G.G., 2001. Mechanisms of spreading depression and hypoxic spreading depression-like depolarization. Physiological Reviews 81 (3), 1065–1096.

Somjen, G.G., 2002. Ion regulation in the brain: implications for pathophysiology. Neuroscientist 8 (3), 254–267.

Somjen, G.G., Müller, M., 2000. Potassium-induced enhancement of persistent inward current in hippocampal neurons in isolation and in tissue slices. Brain Research 885 (1), 102–110.

Thompson, R.J., Zhou, N., MacVicar, B.A., 2006. Ischemia opens neuronal gap junction hemichannels. Science 312 (5775), 924–927.

van Harreveld, A., 1978. Two mechanisms for spreading depression in the chicken retina. Journal of Neurobiology 9 (6), 419–431.

Walz, W., 1987. Swelling and potassium uptake in cultured astrocytes. Canadian Journal of Physiology and Pharmacology 65 (5), 1051–1057.

Wu, J., Fisher, R.S., 2000. Hyperthermic spreading depressions in the immature rat hippocampal slice. Journal of Neurophysiology 84 (3), 1355–1360.

Xiong, Z.Q., Stringer, J.L., 2000. Sodium pump activity, not glial spatial buffering, clears potassium after epileptiform activity induced in the dentate gyrus. Journal of Neurophysiology 83 (3), 1443–1451.